



Anion channel sensitivity to cytosolic organic acids implicates a central role for oxaloacetate in integrating ion flux with metabolism in stomatal guard cells

Yizhou Wang, Michael R. Blatt

► To cite this version:

Yizhou Wang, Michael R. Blatt. Anion channel sensitivity to cytosolic organic acids implicates a central role for oxaloacetate in integrating ion flux with metabolism in stomatal guard cells. *Biochemical Journal*, 2011, 439 (1), pp.161-170. <10.1042/BJ20110845>. <hal-00628679>

HAL Id: hal-00628679

<https://hal.science/hal-00628679v1>

Submitted on 4 Oct 2011

HAL is a multi-disciplinary open access archive for the deposit and dissemination of scientific research documents, whether they are published or not. The documents may come from teaching and research institutions in France or abroad, or from public or private research centers.

L'archive ouverte pluridisciplinaire **HAL**, est destinée au dépôt et à la diffusion de documents scientifiques de niveau recherche, publiés ou non, émanant des établissements d'enseignement et de recherche français ou étrangers, des laboratoires publics ou privés.



HAL Authorization

Research Paper

**ANION CHANNEL SENSITIVITY TO CYTOSOLIC ORGANIC ACIDS
IMPLICATES A CENTRAL ROLE FOR OXALOACETATE IN INTEGRATING ION
FLUX WITH METABOLISM IN STOMATAL GUARD CELLS**

Yizhou Wang and Michael R. Blatt*

Laboratory of Plant Physiology and Biophysics, Institute of Molecular Cell and Systems
Biology, Bower Building, University of Glasgow, Glasgow G12 8QQ UK

*Author for correspondence; phone +44 (0)141 330 4771, email Michael.Blatt@glasgow.ac.uk

Running Head: Anion channel sensitivity to organic acids

Abbreviations used: Ac, acetate; $[Ca^{2+}]_i$, cytosolic-free Ca^{2+} concentration; I_{Cl} , anion (channel)
current; Mal, malate; OAA, oxaloacetate; TEA, tetraethylammonium

SYNOPSIS

Stomatal guard cells play a key role in gas exchange for photosynthesis and in minimizing transpirational water loss from plants by opening and closing the stomatal pore. The bulk of the osmotic content driving stomatal movements depends on ionic fluxes across both the plasma membrane and tonoplast, the metabolism of organic acids, primarily malate (Mal), its accumulation and loss. Anion channels at the plasma membrane are thought to comprise a major pathway for Mal efflux during stomatal closure, implicating their key role in linking solute flux with metabolism. Nonetheless, little is known of the regulation of anion channel current (I_{Cl}) by cytosolic malate or its immediate metabolite oxaloacetate (OAA). We have examined the impact of Mal, OAA, and of the monocarboxylic acid anion acetate in guard cells of *Vicia faba* L. and report that all three organic acids affect I_{Cl} , but with markedly different characteristics and sidedness to their activities. Most prominent was a suppression of I_{Cl} by OAA within the physiological range of concentrations found in vivo. These findings indicate a capacity for OAA to coordinate organic acid metabolism with I_{Cl} through the direct effect of organic acid pool size. Our findings also add perspective to in vivo recordings using acetate-based electrolytes.

Keywords: Stomatal guard cell / stomatal movement, diurnal / organic acid metabolism / anion channel, voltage-gated / voltage clamp / Ca^{2+} concentration, cytosolic-free

INTRODUCTION

Stomata are pores that provide the major route for gas exchange across the impermeable cuticle of leaves and stems [1]. They open and close in response to exogenous and endogenous signals and thereby control the exchange of gases, most importantly water vapour and CO₂, between the interior of the leaf and the atmosphere. The guard cells surrounding the stomatal pore respond to a number of well-defined signals – including hormones, light and atmospheric CO₂ concentration – integrating these signals to regulate stomatal aperture and balance the conflicting needs for water conservation and for inorganic carbon for photosynthesis. The acquisition of stomata and the leaf cuticle are considered to be key elements in the evolution of advanced terrestrial plants [2] as these adaptations allow the plant to inhabit a range of different, often fluctuating environments, and still control water content.

A very large body of experimental evidence supports the central role of ionic fluxes, across both the plasma membrane and tonoplast, and of metabolism, notably of organic acids including malate, in collectively shaping the cyclical changes in osmotic load and turgor pressure that drive guard cells to open and close the stomatal pore [1,3-6]. At maturity, stomatal guard cells lack plasmodesmatal connections with the neighbouring epidermal cells [7]. Thus, guard cells define a semi-closed cellular system within the surrounding leaf tissue. Transport of all inorganic ions – K⁺ and Cl⁻, both major contributors to the osmotic content of guard cells, along with H⁺ and Ca²⁺ – takes place across the plasma membrane and coordinates with the metabolism of osmotically-active organic compounds.

At the plasma membrane, anion channels are key elements that contribute to stomatal closing, and their activities are essential to depolarise the membrane and balance charge with K⁺ during solute efflux for stomatal closure [3,4,8]. The guard cell anion channels divide between two major groupings, based on their physiological characteristics. The slow, or S-type anion channels were originally identified with a slow-activating and largely voltage-independent current that is strongly activated by cytosolic-free [Ca²⁺] ([Ca²⁺]_i) in the micromolar range [9,10]; these channels have since been associated with the *SLAC1* gene product in the model plant *Arabidopsis* [11,12]. The rapid, or R-type anion channels were first characterised by a strongly voltage-dependent current that activated on increasing membrane voltage beyond the range of -100 to -80 mV and inactivated within a few tens to hundreds of milliseconds at more negative voltages [9,13,14].

Both anion channels are closely tied to malate (Mal), contributing to its homeostasis and most likely to its release to the apoplast during stomatal closing [15,16]. The *slac1* loss-of-function mutation is associated with over-accumulations of Mal and other organic acids as well as K⁺ [12] and very high cytosolic concentrations of Mal may itself inhibit the SLAC1 current [17]. The molecular identity of the R-type anion channels remains uncertain, but it has been suggested that ALMT12 and other members of this aluminum-activated Mal transporter family may contribute to the anion current in *Arabidopsis* [18]. Indeed, extracellular malate alters the voltage dependence of R-type anion channels [14] and similarly of current associated with AtALMT12 [18], in effect promoting anion efflux through the channels in response to the organic anion outside. These observations have been interpreted as an indirect ‘feedforward’ mechanism for CO₂ control of the channels [14], but the implied consequences of the related input from the cytosolic metabolites have been largely ignored.

We have explored the ensemble anion channel current, hereafter designated as I_{Cl}, and its regulation by metabolically-related organic acid anions through experimental manipulations both outside and inside guard cells of *Vicia faba* L., the broadbean plant widely used as a model in physiological studies of guard cells. We report that Mal action shows a pronounced biphasic characteristic, with higher Mal concentrations outside suppressing I_{Cl}. We

also find that Mal as well as its precursor oxaloacetate (OAA) suppress I_{Cl} in a voltage-independent manner when present on the cytosolic side of the membrane, the effect of OAA evident well-within its physiological concentration range. These findings point to control of the anion channels by OAA, indicating the capacity for feedback control from the cellular metabolic activity and a much more subtle ‘fine tuning’ of the anion channels by metabolism than previously anticipated.

MATERIAL AND METHODS

Plant growth and preparation

Vicia faba L. cv. Bunyard Exhibition was grown on potting mix and perlite (70:30) at 22° C and 60% relative humidity with 200 $\mu\text{mol m}^{-2} \text{sec}^{-1}$ photosynthetic photon flux density under a 16/8 h day/night cycle. Epidermal strips were prepared from newly expanded leaves of 4- to 6-week-old plants as described previously [19]. Epidermal peels were affixed to the glass bottom of the experimental chamber after coating the chamber surface with an optically clear and pressure-sensitive silicone adhesive and all operations were carried out on an Axiovert S100TV microscope (Zeiss, Oberkochen, Germany) fitted with Nomarski differential interference contrast optics. Measurements were conducted in continuous flowing solutions controlled by a gravity-fed system at a rate of 20 chamber volumes min^{-1} . The standard perfusion medium contained 15 mM TEA-Cl, 15 mM CsCl and 5 mM 2-(N-morpholino)propanesulphonic acid (MES), titrated with $\text{Ca}(\text{OH})_2$ to pH 6.1 ($[\text{Ca}^{2+}] = 1 \text{ mM}$). The Na^+ salts of organic acids and other chemicals were from Sigma (Poole, UK) unless otherwise specified.

Electrophysiology

Surface area and volume of impaled epidermal cells were calculated assuming a cylindrical geometry using Henry IV EP software (www.psrg.org.uk/Software/Henry.htm). Single and double-barrelled microelectrodes were prepared and coated with paraffin to reduce capacitance as described previously [19-21]. Current- and voltage-recording barrels were filled with 100 mM CsCl with additions as indicated. For measurements including organic acids in the microelectrode, K^+ salts of the acids were used and the electrolyte solution was adjusted to pH 7.5 with CsOH and HCl as necessary to avoid cytosolic acid or alkaline loading. Microelectrodes were connected to amplifier headstages via 1 M KCl | Ag-AgCl halfcells, and a 1 M KCl agar bridge served as the reference electrode. Voltage clamp recordings were carried out using Henry IV EP software using a two-electrode clamp circuit [20,21] with an additional μP amplifier (Y-Science). Current records were filtered using an eight-pole active Bessel filter (f_c , 0.3 kHz) and clamp current and voltage data were digitized at 1 kHz. Free-running voltages between voltage clamp recordings were digitized at 10 Hz.

Numerical analyses

All recordings were analyzed and leak currents subtracted using standard methods [21] with Henry IV software. Where appropriate data are presented as means \pm SE of n observations, and differences validated by Student's T-test or ANOVA. Curve fittings were by nonlinear least-squares using a Marquardt-Levenberg algorithm [22].

RESULTS

Previous studies indicated an activation of anion currents by extracellular Mal in isolated protoplasts [14], but supporting evidence from intact guard cells has been equivocal [23]. We recorded I_{Cl} with a two-electrode voltage clamp in intact guard cells, bathing the cells in 15 mM CsCl and 15 mM tetraethylammonium chloride (TEA-Cl), and using microelectrodes filled with 100 mM CsCl. Diffusion of Cs^+ from the microelectrode and its presence with TEA^+ outside blocks all K^+ currents and Cl^- diffusion from the microelectrode provides an effective 'substrate clamp' loading the cytosol within the first 5-10 min following impalements to enhance current carried by the anion [24-26]. Under these conditions, the membrane was dominated by I_{Cl} similar to that reported previously with instantaneous current comprising both anion channels and characteristics in the steady-state predominantly of the S-type anion current [9,26,27].

Biphasic activation of I_{Cl} by external Mal

To test the effects of Mal outside, after impalements we superfused guard cells with malate concentrations up to 20 mM. Figure 1A summarises results from 10 independent experiments, for clarity showing data only for the 0, 1 and 10 mM Mal, including recordings from one guard cell at the three Mal concentrations (*insets below*). Clamp voltage steps to +40 mV led to a slow rise in outward current over 10 s (not shown), and subsequent clamp steps to voltages negative of approximately -40 mV yielded substantial inward-directed and instantaneous I_{Cl} that relaxed to steady-state values near -5 to -10 $\mu A\ cm^{-2}$ within 3-5 s. Both mean instantaneous and, to a lesser extent, steady-state (*inset above*) I_{Cl} were enhanced by 1 mM Mal. Amplitudes of the mean instantaneous current increased by 70-75% at voltages negative from -100 mV (from -52 ± 7 to $-91 \pm 9\ \mu A\ cm^{-2}$ at -220 mV) and near the negative maximum at -75 mV the mean steady-state current increased by approximately 60% from -13 ± 1 to $-22 \pm 3\ \mu A\ cm^{-2}$. Analogous to previous results [14], we observed roughly a -30 mV displacement in the voltage giving maximum steady-state I_{Cl} in 1 mM Mal and a marginally greater displacement in 10 mM Mal (*inset above*). However, in 10 mM Mal both instantaneous and steady-state I_{Cl} were reduced close to control values in the absence of Mal, and similar results were obtained with 20 mM Mal (not shown). To assess further Mal action on I_{Cl} gating, we fitted I_{Cl} relaxations to derive the half-time, $t_{1/2}$, for current deactivation at voltages negative of -40 mV for all three sets of data. Figure 1B shows the voltage-dependence of $t_{1/2}$ for I_{Cl} [26] and underscores the biphasic action of Mal on the current: whereas 1 mM Mal resulted in an increase in $t_{1/2}$ consistent with a slowing of its relaxation, especially at more negative voltages (*inset*), additions of 10 mM Mal yielded $t_{1/2}$ values statistically indistinguishable from the control at all voltages.

Cytosolic Mal suppresses I_{Cl}

Although implicit in the connection to cellular metabolism, to date almost nothing is known about the influence of Mal on I_{Cl} from the cytosolic side of the membrane. Guard cells of many species, including *Vicia*, accumulate high concentrations of Mal to balance K^+ uptake during stomatal opening [6,16,28]. Much of this Mal is distributed to the vacuole, but concentrations of 1-8 mM have been estimated in the cytosol [6,29]. To examine the effect of Mal on I_{Cl} from inside, we impaled guard cells with double-barrelled microelectrodes as before, but with concentrations between 1 mM and 20 mM Mal in addition to 100 mM CsCl filling the microelectrode barrels to load the cytosol by diffusion from the microelectrode. Figure 2 summarises data from 10 or more independent experiments with each loading solution, in each case allowing at least 10 min following impalements for loading from the microelectrode [24-26]. Recordings from guard cells impaled with 1 mM Mal in the microelectrodes showed a statistically significant increase in I_{Cl} between -40 mV and -100 mV in the steady-state (Fig. 2A),

but the effect on the instantaneous current amplitude was marginal (*inset*) and no effect was evident in mean $t_{1/2}$ values for I_{Cl} deactivation at any voltage (Fig. 2B). By contrast, recordings from guard cells impaled with 10 mM Mal in the microelectrodes yielded a reduction in instantaneous I_{Cl} compared to the control, albeit with a smaller effect on the steady-state current (Fig. 2A) and greatly reduced $t_{1/2}$ (Fig. 2B) independent of membrane voltage. Similar results were obtained with 20 mM Mal (not shown), and fittings to a hyperbolic function for the $t_{1/2}$ and amplitude of I_{Cl} (see Fig. 8) yielded apparent K_s s for Mal of 3 ± 1 mM and 10 ± 3 mM, respectively. Thus, Mal suppressed I_{Cl} on transition to negative voltages, accelerating deactivation and reducing the magnitude of the current, but the effect on current amplitude was evident primarily at the upper end of the physiological range of Mal concentrations.

Cytosolic oxaloacetate blocks I_{Cl}

Oxaloacetate (OAA) is the four-carbon precursor in the formation of cytosolic malate from phosphoenolpyruvate and immediate product of malate oxidation; it is an intermediate in several metabolic pathways – including glycolysis, amino acid synthesis and in the mitochondrial tricarboxylic acid cycle – and it exchanges with malate across both chloroplast and mitochondrial membranes [6,29]. Direct measurements of steady-state OAA concentration in the cytosol are not available, but estimates based on energy charge and Mal/OAA exchange transport equilibria suggest values of 0.1–0.5 mM and possibly as high as 3 mM in the light [30]. Given its central importance to Mal balance, we examined the effects on I_{Cl} of OAA additions both outside and inside the guard cells. We found that OAA concentrations as high as 10 mM added outside had no appreciable effect on instantaneous or steady-state I_{Cl} (Fig. 3A), nor did it alter channel gating when quantified using current relaxations on deactivation at negative voltages (Fig. 3B). By contrast, cytosolic OAA loads introduced from the microelectrodes had a substantial effect on all three parameters. Adding 1 and 10 mM OAA inside suppressed the instantaneous I_{Cl} approximately 58% and 70%, respectively, compared to the control and independent of membrane voltage (Fig. 4A). A similar block of steady-state I_{Cl} was observed in each case (Fig. 4A, *inset*) and I_{Cl} kinetics showed a substantial acceleration in current deactivation, notable even with 1 mM OAA and again largely independent of membrane voltage (Fig. 4B). Fitting to a hyperbolic function (see Fig. 8) yielded apparent K_s s for OAA in accelerating I_{Cl} deactivation and reducing the current amplitude of 0.17 ± 0.08 mM and 0.21 ± 0.05 mM, respectively, that is well within the physiological range of OAA concentrations. Additions of OAA, both inside and outside the guard cells had no significant effect on the reversal voltage for I_{Cl} – as evidenced by a lack of significant difference in currents recorded either side of the apparent reversal voltage (see Fig. 4 legend) – indicating that the relative permeability of the channels for OAA is very low compared to that for Cl^- and Mal.

Given the potentially counteractive effects of the organic acids in the cytosol we also examined whether OAA suppression of I_{Cl} was rescued in the presence of Mal. In this case, guard cells were impaled with microelectrodes containing 1 mM OAA and 1 mM Mal and I_{Cl} recorded as before. Figure 5 summarises results from 11 independent experiments with both organic acids. We found that OAA suppressed both instantaneous and steady-state I_{Cl} (Fig. 5A) and accelerated current deactivation (Fig. 5B). This effect was only partially ameliorated by the presence of low Mal concentrations that enhanced I_{Cl} (see Fig. 2) and, again, the influence of both organic acids was voltage independent (Fig. 5B, *inset*). These results suggest that the immediate metabolic partner of Mal may have an important role in control of I_{Cl} under normal physiological conditions.

Acetate electrolytes impact on I_{Cl}

Finally, we explored the impact of acetate (Ac) on I_{Cl} . The two-carbon acid anion is a substrate for the tricarboxylic acid cycle and fatty acid synthesis, but in a thioester complex with Coenzyme A and normally occurs as the free acid at concentrations of 0.5-1.5 mM [31]. Nonetheless, previous electrophysiological studies have used the free acid anion in microelectrode filling solutions to avoid cytosolic Cl^- loading and its consequences for solute balance and background Cl^- leakage across the membrane [24,25,32-34]. In the absence of information on the Ac-sensitivity of I_{Cl} , we challenged guard cells with 1 and 10 mM Ac by additions outside and to the microelectrode filling solution. Figures 6 and 7 summarise results of 13 or more independent experiments for each treatment. We found in every case that increasing Ac concentrations suppressed the instantaneous and steady-state I_{Cl} , in the latter case most noticeably at voltages between -40 and -100 mV, and it accelerated current deactivation. Unlike the effects of Mal and OAA, however, Ac showed a pronounced voltage dependence in its effect on I_{Cl} kinetics, the reduction in $t_{1/2}$ being most apparent at voltages near and positive of -100 mV and when Ac was added to the cytosolic side of the membrane (Figs. 6B and 7B), and it led to a shift in the apparent reversal potential for I_{Cl} (Fig. 6A and 7A, *insets*). These results indicate a more complex interaction of Ac with the anion channels and we return to this point below.

DISCUSSION

Both inorganic ion transport and organic acid metabolism make major contributions to the changes in osmotic content of the guard cells that drives stomatal movements [3,4,35,36]. During the diurnal cycle of stomatal opening and closing, the guard cells of most plant species accumulate and subsequently lose significant quantities of K^+ , Cl^- and Mal, the latter offsetting Cl^- especially later in the daylight period [16,37-39]. Much of the Mal synthesized in the light is transported and accumulates in the vacuole [29], but is later transported out of the vacuole to be metabolised or released across the plasma membrane when the stomata close [28,40]. Thus transport, notably of Cl^- and Mal, must be regulated in concert with metabolism, both as Mal is synthesized for transport to the vacuole and again as it re-enters the cytosol for export and to feed into the metabolic pools of other organic acids. Very little is known of the mechanisms behind this regulation, although it is clearly central to the osmotic homeostasis of guard cells. We have examined the impact of cytosolic Mal, its immediate metabolite OAA, and of Ac on I_{Cl} , the current carried by anion channels at the plasma membrane of *Vicia* guard cells. Although we cannot discount some degree of metabolic conversion of the acid anions during these experiments, both the extracellular medium and the microelectrode present virtually infinite volumes, the latter exchanging with the cytosol directly. Thus, at steady-state the membrane surface will have been exposed to organic acid concentrations effectively 'clamped' close to that of the corresponding solutions [24,25]. We found that all three organic acids affected I_{Cl} , but with markedly different characteristics and sidedness to their activities. Most prominent was the suppression of I_{Cl} with OAA evident even at low millimolar concentrations. These findings indicate a capacity for coordinating organic acid metabolism with I_{Cl} through the direct effect of organic acid pool size and they suggest that the effects may be exerted as much by Mal metabolites as by Mal itself. They also add perspective to in vivo recordings using Ac-based electrolytes.

Malate, oxaloacetate and I_{Cl} regulation

One of the most surprising of our findings was that I_{Cl} is substantially more sensitive to OAA in the cytosol than it is to Mal (Fig. 8). Much as previously reported [14,17], we observed that low concentrations of Mal outside affected the voltage dependence of the current. We also observed an enhancement of I_{Cl} with 1 mM Mal in the cytosol, although elevation of cytosolic Mal to 10-20 mM led to measurable declines in I_{Cl} relative to the control (Fig. 2). Additions even of 1 mM OAA, however, resulted in a significant block of I_{Cl} consistent with an apparent K_i near 0.1 mM and well within the dynamic concentration range for OAA in vivo [30]. Mal synthesis in the cytosol of guard cells is fed largely from the pools of phosphoenolpyruvate and OAA [6]. The flux through these metabolites will be balanced in part with Mal transport across the tonoplast and can lead to large accumulations of Mal in the vacuole especially in the second half of the diurnal cycle [6,37]. By contrast, stomatal closure at the end of the day or following stimulation with abscisic acid must be accompanied by export of much of the Mal in the vacuole and its elimination through metabolism and loss across the plasma membrane [6,35]. These observations are generally consistent with variations in the low millimolar range previously reported for the pool of cytosolic Mal in leaves [29]. However, such 'channelling' of Mal, in the first instance into the vacuole and in the second to the apoplast, implies a substantial hysteresis in Mal flux control overall and a fine control over Mal export both at the tonoplast and at the plasma membrane during the course of the day.

If the cytosolic Mal pool remains within the bounds of 0.5-10 mM, how might I_{Cl} be regulated to prevent undue Mal efflux during stomatal opening yet provide a major pathway for its loss during stomatal closure? One obvious mechanism rests with increasing $[Ca^{2+}]_i$ that

enhance the activity of I_{Cl} and both R- and S-type anion channels [9,14,27,41,42], in effect promoting Mal (and Cl^-) efflux across the plasma membrane. This mechanism is certainly important in the response of guard cells to ABA and drought stress [3,4], but it is more difficult to reconcile the diurnal cycle of $[Ca^{2+}]_i$ with that of Mal synthesis and accumulation in the day and release at night. Guard cells undergo diurnal changes in $[Ca^{2+}]_i$, but the range of free concentrations in the steady-state [43,44] is substantially below the $K_{1/2}$ of 600-700 nM for I_{Cl} activation by $[Ca^{2+}]_i$ [27]. Furthermore, the diurnal oscillation in $[Ca^{2+}]_i$ is 180° out of phase with the changes that might be expected to modulate Mal in guard cells [44]: $[Ca^{2+}]_i$ increases in the day and declines at night, whereas the opposite would be required to facilitate Mal accumulation in the day and its efflux through the anion channels at night. In short, the diurnal changes in Mal do not sit well with the characteristics of I_{Cl} modulation by $[Ca^{2+}]_i$ in guard cells.

The sensitivity of I_{Cl} to OAA does lend itself to another mechanism however. It is generally thought that much of the fixed carbon in guard cells is imported and passes through glycolysis before condensation with bicarbonate to form OAA and Mal [6,45,46]. OAA is formed through the action of phosphoenol pyruvate carboxylase, which activated by its phosphorylation in the light thus suppressing its sensitivity to inhibition by Mal [47,48]. Thus, we might anticipate that sucrose uptake and metabolism to form Mal in the light will be accompanied by an elevation in the cytosolic OAA pool, even if NAD-malate dehydrogenase is activated by light [49]; conversely, carbon passage through Mal and OAA to PEP and pyruvate and transfer of both Mal and pyruvate to the mitochondria at the end of the day [6] is likely to be accompanied by a relative depletion of this same OAA pool. In other words, diurnal variations in cytosolic OAA are potentially in phase with the expected oscillation between Mal retention and stomatal opening during the day and I_{Cl} -mediated Mal release and stomatal closure at night. The K_m for OAA of cytosolic NAD-malate dehydrogenase [49] is very close to the apparent K_i for OAA of I_{Cl} in *Vicia* guard cells (Figs. 4 and 8), thereby ensuring a close coordination between the two kinetic processes. We note, too, that low millimolar OAA inside suppresses I_{Cl} even in the presence of Mal (Figs. 4 and 5). So it is conceivable that diurnal variations in the cytosolic OAA could play an important role in regulating I_{Cl} and Mal efflux across the plasma membrane. Indeed, in this context it is of interest to note that the diurnal oscillation of the OAA pool in various CAM species is also in phase with stomatal movements [50], albeit with the higher OAA concentration and stomatal opening at night.

Electrophysiological studies with acetate electrolytes

Finally it is of interest that I_{Cl} showed a sensitivity to Ac. The monocarboxylic acid is normally present at low concentrations [31] relative to its action on the current (Figs. 6 and 7), and is therefore unlikely to have an impact on I_{Cl} activity in vivo. Effects of weak-acid loading with Ac can also be ruled out because, counter to the the evidence of Figs. 6 and 7, cytosolic acidification enhances anion channel activity [51]. The action of higher Ac concentrations is relevant, however, because the caboxylic acid anion is commonly used as an electrolyte substitute to avoid the consequences of Cl^- loading via the microelectrode [24,25,32-34]. It is clear that this practice does more than simply avoiding the effects of elevating Cl^- in the cytosol: Ac loading leads to a block of I_{Cl} . Our results – including parallel effects for Ac added outside and inside, the apparent shift in instantaneous current and current reversal voltage, and the strong voltage dependence to its action on $t_{1/2}$ (Figs. 6 and 7) – implies a complex dependence on Ac residence within the channel pore itself; furthermore, the voltage-dependence to Ac action (Figs. 6B and 7B) and the more pronounced effect on instantaneous I_{Cl} when added outside (Fig. 6A) may indicate a greater sensitivity of the R-type anion channels to Ac. Regardless, however, the block of I_{Cl} has had the serendipitous advantage of simplifying the kinetic analysis of the guard

cell K^+ channels and other currents through their isolation from anion flux through I_{Cl} .

From a physiological standpoint, the block of I_{Cl} by Ac will not influence other membrane currents under voltage clamp. However, it may well affect the balance of ionic currents under free-running (non-clamped) conditions. For example, suppressing I_{Cl} might be expected to promote Ca^{2+} entry and $[Ca^{2+}]_i$ elevation initially by favouring membrane hyperpolarisation, even with low millimolar concentrations of K^+ outside [4,8,52]. Raising $[Ca^{2+}]_i$ above 500-600 nM normally promotes a burst in I_{Cl} activity [27], but this activity is likely to be much suppressed by an Ac load with a consequent loss of the 'damping' effect of I_{Cl} in promoting membrane depolarisation. In short, Ac loading may have led to an overestimate of the normal dynamic range for $[Ca^{2+}]_i$ in its coupling with oscillations with membrane voltage [53,54]. Indeed, preliminary analysis using quantitative kinetic modelling of guard cell ion transport and homeostasis has suggested that $[Ca^{2+}]_i$ oscillations are likely to be constrained with an upper limit near 600 nM largely as a result of I_{Cl} activation [55].

In conclusion, we find that the anion channel current of *Vicia* guard cells shows a compound dependence, from the cytosolic side of the membrane, on several organic acids. Most notable, suppression of I_{Cl} by OAA is consistent with a role for this dicarboxylic acid in modulating channel activity for a diurnal cycle of Mal accumulation and release that parallels the cycle of stomatal opening and closing. Additionally, block of I_{Cl} by the monocarboxylic acid Ac demonstrates that its use in electrophysiological studies has serendipitous consequences for the study of other ion channels at the guard cell plasma membrane.

Acknowledgements

We thank Amparo Ruiz-Prado for preparing plant materials and Dr. Zhonghua Chen for helpful discussion during the preparation of the manuscript. This work was supported by BBSRC grants BB/F001673/1 and BB/F001630/1 to MRB. YW is holds China Scholarship Council Studentship with the University of Glasgow.

References:

- 1 Hetherington, A.M. and Woodward, F.I. (2003) The role of stomata in sensing and driving environmental change. *Nature*, **424**, 901-908.
- 2 Raven, J.A. (2002) Selection pressures on stomatal evolution. *New Phytol.*, **153**, 371-386.
- 3 Schroeder, J.I., Allen, G.J., Hugouvieux, V., Kwak, J.M. and Waner, D. (2001) Guard cell signal transduction. *Ann. Rev. Plant Physiol. Mol. Biol.*, **52**, 627-658.
- 4 Blatt, M.R. (2000) Cellular signaling and volume control in stomatal movements in plants. *Ann. Rev. Cell Dev. Biol.*, **16**, 221-241.
- 5 Sokolovski, S. and Blatt, M.R. (2007) Nitric oxide and plant ion channel control. In *Nitric Oxide in Plant Growth, Development and Stress Physiology* (Lamattina, L. and Polacco, J.C. Eds.), pp. 153-172. Springer, Berlin.
- 6 Willmer, C. and Fricker, M. D. Stomata. 2, 1-375. 1996. London, Chapman and Hall.
- 7 Wille, A. and Lucas, W. (1984) Ultrastructural and histochemical studies on guard cells. *Planta*, **160**, 129-142.
- 8 Pandey, S., Zhang, W. and Assmann, S.M. (2007) Roles of ion channels and transporters in guard cell signal transduction. *FEBS Lett.*, **581**, 2325-2336.
- 9 Schroeder, J.I. and Keller, B.U. (1992) Two types of anion channel currents in guard cells with distinct voltage regulation. *Proc. Natl. Acad. Sci. USA*, **89**, 5025-5029.
- 10 Schroeder, J.I. (1989) Quantitative analysis of outward rectifying K⁺ channel currents in guard cell protoplasts from *Vicia faba*. *J. Membr. Biol.*, **107**, 229-235.
- 11 Negi, J., Matsuda, O., Nagasawa, T., Oba, Y., Takahashi, H., Kawai-Yamada, M., Uchimiya, H., Hashimoto, M. and Iba, K. (2008) CO₂ regulator *SLAC1* and its homologues are essential for anion homeostasis in plant cells. *Nature*, **452**, 483-486.
- 12 Vahisalu, T., Kollist, H., Wang, Y.F., Nishimura, N., Chan, W.Y., Valerio, G., Lamminmaki, A., Brosche, M., Moldau, H., Desikan, R., Schroeder, J.I. and Kangasjarvi, J. (2008) SLAC1 is required for plant guard cell S-type anion channel function in stomatal signalling. *Nature*, **452**, 487-491.
- 13 Hedrich, R., Busch, H. and Raschke, K. (1990) Ca²⁺ and nucleotide dependent regulation of voltage dependent anion channels in the plasma membrane of guard cells. *EMBO J.*, **9**, 3889-3892.
- 14 Hedrich, R. and Marten, I. (1993) Malate-induced feedback regulation of plasma membrane anion channels could provide a CO₂ sensor to guard cells. *EMBO J.*, **12**, 897-901.
- 15 VanKirk, C.A. and Raschke, K. (1978) Release of malate from epidermal strips during stomatal closure. *Plant Physiol.*, **61**, 474-475.

- 16 Raschke, K. and Schnabl, H. (1978) Availability of chloride affects balance between potassium chloride and potassium malate in guard cells of *Vicia faba* L. *Plant Physiol.*, **62**, 84-87.
- 17 Schmidt, C. and Schroeder, J.I. (1994) Anion selectivity of slow anion channels in the plasma membrane of guard cells - large nitrate permeability. *Plant Physiol.*, **106**, 383-391.
- 18 Meyer, S., Mumm, P., Imes, D., Endler, A., Weder, B., Al-Rasheid, K.A.S., Geiger, D., Marten, I., Martinoia, E. and Hedrich, R. (2010) AtALMT12 represents an R-type anion channel required for stomatal movement in *Arabidopsis* guard cells. *Plant J.*, **63**, 1054-1062.
- 19 Blatt, M.R. (1992) K⁺ channels of stomatal guard cells: characteristics of the inward rectifier and its control by pH. *J. Gen. Physiol.*, **99**, 615-644.
- 20 Blatt, M.R. (1987) Electrical characteristics of stomatal guard cells: the contribution of ATP-dependent, "electrogenic" transport revealed by current-voltage and difference-current-voltage analysis. *J. Membr. Biol.*, **98**, 257-274.
- 21 Blatt, M.R. (2004) Concepts and techniques in plant membrane physiology. In *Membrane Transport in Plants* (Blatt, M.R. Ed.), pp. 1-39. Blackwell, Oxford.
- 22 Marquardt, D. (1963) An algorithm for least-squares estimation of nonlinear parameters. *J. Soc. Ind. Appl. Math.*, **11**, 431-441.
- 23 Raschke, K., Shababang, M. and Wolf, R. (2003) The slow and the quick anion conductance in whole guard cells: their voltage-dependent alternation, and the modulation of their activities by abscisic acid and CO₂. *Planta*, **217**, 639-650.
- 24 Blatt, M.R. and Slayman, C.L. (1983) KCl leakage from microelectrodes and its impact on the membrane parameters of a nonexcitable cell. *J. Membr. Biol.*, **72**, 223-234.
- 25 Blatt, M.R. (1987) Electrical characteristics of stomatal guard cells: the ionic basis of the membrane potential and the consequence of potassium chloride leakage from microelectrodes. *Planta*, **170**, 272-287.
- 26 Grabov, A. and Blatt, M.R. (1997) Parallel control of the inward-rectifier K⁺ channel by cytosolic-free Ca²⁺ and pH in *Vicia* guard cells. *Planta*, **201**, 84-95.
- 27 Chen, Z.H., Hills, A., Lim, C.K. and Blatt, M.R. (2010) Dynamic regulation of guard cell anion channels by cytosolic free Ca²⁺ concentration and protein phosphorylation. *Plant J.*, **61**, 816-825.
- 28 VanKirk, C.A. and Raschke, K. (1978) Presence of chloride reduces malate production in epidermis during stomatal opening. *Plant Physiol.*, **61**, 361-364.
- 29 Martinoia, E. and Rentsch, D. (1994) Malate compartmentation - responses to a complex metabolism. *Ann. Rev. Plant Physiol. Mol. Biol.*, **45**, 447-467.
- 30 Heineke, D., Riens, B., Grosse, H., Hoferichter, P., Peter, U., Flugge, U.I. and Heldt, H.W.

- (1991) Redox transfer across the inner chloroplast envelope membrane. *Plant Physiol.*, **95**, 1131-1137.
- 31 Roughan, P.G. (1995) Acetate concentrations in leaves are sufficient to drive in vivo fatty-acid synthesis at maximum rates. *Plant Science*, **107**, 49-55.
- 32 Blatt, M.R., Thiel, G. and Trentham, D.R. (1990) Reversible inactivation of K⁺ channels of *Vicia* stomatal guard cells following the photolysis of caged inositol 1,4,5- trisphosphate. *Nature*, **346**, 766-769.
- 33 Garcia-Mata, C., Gay, R., Sokolovski, S., Hills, A., Lamattina, L. and Blatt, M.R. (2003) Nitric oxide regulates K⁺ and Cl⁻ channels in guard cells through a subset of abscisic acid-evoked signaling pathways. *Proc.Natl.Acad.Sci.USA*, **100**, 11116-11121.
- 34 Roelfsema, M.G. and Prins, H.A. (1997) Ion channels in guard cells of *Arabidopsis thaliana* (L) Heynh. *Planta*, **202**, 18-27.
- 35 Roelfsema, M.R.G. and Hedrich, R. (2005) In the light of stomatal opening: new insights into 'the Watergate'. *New Phytol.*, **167**, 665-691.
- 36 Shimazaki, K.I., Doi, M., Assmann, S.M. and Kinoshita, T. (2007) Light regulation of stomatal movement. *Annual Review of Plant Biology*, **58**, 219-247.
- 37 Talbott, L.D. and Zeiger, E. (1993) Sugar and organic acid accumulation in guard cells of *Vicia faba* in response to red and blue light. *Plant Physiol.*, **102**, 1163-1169.
- 38 Talbott, L.D. and Zeiger, E. (1996) Central roles for potassium and sucrose in guard cell osmoregulation. *Plant Physiol.*, **111**, 1051-1057.
- 39 Asai, N., Nakajima, N., Kondo, N. and Kamada, H. (1999) The effect of osmotic stress on the solutes in guard cells of *Vicia faba* L. *Plant Cell Physiol.*, **40**, 843-849.
- 40 Dittrich, P. and Raschke, K. (1977) Malate metabolism in isolated epidermis of *Commelina communis* L. in relation to stomatal functioning. *Planta*, **134**, 77-81.
- 41 Grabov, A., Leung, J., Giraudat, J. and Blatt, M.R. (1997) Alteration of anion channel kinetics in wild-type and *abi1-1* transgenic *Nicotiana benthamiana* guard cells by abscisic acid. *Plant J.*, **12**, 203-213.
- 42 Geiger, D., Scherzer, S., Mumm, P., Marten, I., Ache, P., Matschi, S., Liese, A., Wellmann, C., Al-Rasheid, K.A.S., Grill, E., Romeis, T. and Hedrich, R. (2010) Guard cell anion channel SLAC1 is regulated by CDPK protein kinases with distinct Ca²⁺ affinities. *Proc.Natl.Acad.Sci.USA*, **107**, 8023-8028.
- 43 Dodd, A.N., Gardner, M.J., Hotta, C.T., Hubbard, K.E., Dalchau, N., Love, J., Assie, J.M., Robertson, F.C., Jakobsen, M.K., Goncalves, J., Sanders, D. and Webb, A.A.R. (2007) The *Arabidopsis* circadian clock incorporates a cADPR-based feedback loop. *Science*, **318**, 1789-1792.

- 44 Dodd, A.N., Love, J. and Webb, A.A.R. (2005) The plant clock shows its metal: circadian regulation of cytosolic free Ca^{2+} . *Trends Plant Sci.*, **10**, 15-21.
- 45 Asai, N., Nakajima, N., Tamaoki, M., Kamada, H. and Kondo, N. (2000) Role of malate synthesis mediated by phosphoenolpyruvate carboxylase in guard cells in the regulation of stomatal movement. *Plant Cell Physiol.*, **41**, 10-15.
- 46 Outlaw, W.H. (2003) Integration of cellular and physiological functions of guard cells. *Critical Reviews In Plant Sciences*, **22**, 503-529.
- 47 Outlaw, W.H., Du, Z.R., Meng, F.X., Aghoram, K., Riddle, K.A. and Chollet, R. (2002) Requirements for activation of the signal-transduction network that leads to regulatory phosphorylation of leaf guard-cell phosphoenolpyruvate carboxylase during fusicoccin-stimulated stomatal opening. *Archives of Biochemistry and Biophysics*, **407**, 63-71.
- 48 Cotellet, V., Pierre, J.N. and Vavasseur, A. (1999) Potential strong regulation of guard cell phosphoenolpyruvate carboxylase through phosphorylation. *J.Exp.Bot.*, **50**, 777-783.
- 49 Gotow, K., Tanaka, K., Kondo, N., Kobayashi, K. and Syono, K. (1985) Light activation of NADP-malate dehydrogenase in guard cell protoplasts from *Vicia faba* L. *Plant Physiol.*, **79**, 829-832.
- 50 Chen, L.S., Lin, Q. and Nose, A. (2002) A comparative study on diurnal changes in metabolite levels in the leaves of three crassulacean acid metabolism (CAM) species, *Ananas comosus*, *Kalanchoe daigremontiana* and *K. pinnata*. *J.Exp.Bot.*, **53**, 341-350.
- 51 Schulzlessdorf, B., Lohse, G. and Hedrich, R. (1996) GCAC1 recognizes the pH gradient across the plasma membrane: a pH-sensitive and ATP-dependent anion channel links guard cell membrane potential to acid and energy metabolism. *Plant J.*, **10**, 993-1004.
- 52 Blatt, M.R. and Thiel, G. (1993) Hormonal control of ion channel gating. *Ann.Rev.Plant Physiol.Mol.Biol.*, **44**, 543-567.
- 53 Grabov, A. and Blatt, M.R. (1998) Membrane voltage initiates Ca^{2+} waves and potentiates Ca^{2+} increases with abscisic acid in stomatal guard cells. *Proc.Natl.Acad.Sci.USA*, **95**, 4778-4783.
- 54 Sokolovski, S., Hills, A., Gay, R., Garcia-Mata, C., Lamattina, L. and Blatt, M.R. (2005) Protein phosphorylation is a prerequisite for intracellular Ca^{2+} release and ion channel control by nitric oxide and abscisic acid in guard cells. *Plant J.*, **43**, 520-529.
- 55 Hills, A., Chen, Z.H., Lew, V.L. and Blatt, M.R. (2010) Quantitative Dynamic Systems Modelling of Guard Cell Membrane Transport. *International Plant Membrane Biology Workshop*, **15**, W2-3.

Figure legends:

Fig. 1. External Mal shows a biphasic modulation of I_{Cl} in *Vicia* guard cells.

(A) Instantaneous anion current as a function of voltage from 10 independent experiments as means \pm SE. Measurements were carried out in 5 mM Ca^{2+} -MES buffer, pH 6.1, with 15 mM TEA-Cl and 15 mM CsCl alone and with additions of 1-20 mM Mal. Data for 0 (●), 1 (○) and 10 mM (▼) Mal only shown for clarity. Voltages clamped from a conditioning voltage of +40 mV to voltages between +40 and -220 mV in 10-s steps. *Inset (below)*: representative current traces with 0 indicated on left. Scale: 50 $\mu A\ cm^{-2}$ (vertical), 5 s (horizontal). *Inset (above)*: Steady-state current-voltage curves derived from the same measurements (cross-referenced by symbol).

(B) Current relaxation halftimes ($t_{1/2}$) as a function of voltage. Bars are means \pm SE from the same 10 independent experiments (above) for 0 mM (solid), 1 mM (open) and 10 mM Mal (diagonal-hashed). *Inset*: Relaxation halftimes plotted relative to the control without Mal for 1 mM (●) and 10 mM (○) Mal.

Fig. 2. Internal Mal shows a marginal stimulation of I_{Cl} at low millimolar concentrations in *Vicia* guard cells.

(A) Steady-state anion current as a function of voltage as means \pm SE from 10 or more independent experiments at each Mal concentration. Measurements were carried out in 5 mM Ca^{2+} -MES buffer, pH 6.1, with 15 mM TEA-Cl and 15 mM CsCl. Guard cells were impaled with double-barrelled microelectrodes filled with 100 mM CsCl alone (●) and with additions 1-20 mM Mal; data for 1 mM (○) and 10 mM (▼) Mal only shown for clarity (see also Fig. 8). Voltages clamped from a conditioning voltage of +40 mV to voltages between +40 and -220 mV in 10-s steps as in Fig. 1. *Inset (above)*: Instantaneous current-voltage curves derived from the same measurements (cross-referenced by symbol).

(B) Current relaxation halftimes ($t_{1/2}$) as a function of voltage. Bars are means \pm SE from the same experiments (above) for 0 mM (solid), 1 mM (open) and 10 mM Mal (diagonal-hashed). *Inset*: Relaxation halftimes plotted relative to the control without Mal for 1 mM (●) and 10 mM (○) Mal.

Fig. 3. I_{Cl} in *Vicia* guard cells shows no appreciable sensitivity to external OAA.

(A) Instantaneous anion current as a function of voltage from 15 independent experiments as means \pm SE. Measurements were carried out in 5 mM Ca^{2+} -MES buffer, pH 6.1, with 15 mM TEA-Cl and 15 mM CsCl alone and with additions of 1-10 mM OAA. Data for 0 (●), 1 (○) and 10 mM (▼) Mal only shown for clarity. Voltages clamped from a conditioning voltage of +40 mV to voltages between +40 and -220 mV in 10-s steps as in Fig. 1. *Inset (above)*: Steady-state current-voltage curves derived from the same measurements (cross-referenced by symbol).

(B) Current relaxation halftimes ($t_{1/2}$) as a function of voltage. Bars are means \pm SE from the same experiments (above) for 0 mM (solid), 1 mM (open) and 10 mM Mal (diagonal-hashed). *Inset*: Relaxation halftimes plotted relative to the control without OAA for 1 mM (●) and 10 mM (○) OAA.

Fig. 4. Internal OAA suppresses I_{Cl} at low millimolar concentrations in *Vicia* guard cells.

(A) Instantaneous anion current as a function of voltage as means \pm SE from 10 or more independent experiments at each OAA concentration. Measurements were carried out in 5 mM Ca^{2+} -MES buffer, pH 6.1, with 15 mM TEA-Cl and 15 mM CsCl. Guard cells were impaled with double-barrelled microelectrodes filled with 100 mM CsCl alone (●) and with

additions 1-10 mM OAA; data for 1 mM (○) and 10 mM (▼) Mal only shown for clarity (see also Fig. 8). Voltages clamped from a conditioning voltage of +40 mV to voltages between +40 and -220 mV in 10-s steps as in Fig. 1. Statistical analysis by ANOVA indicated that currents recorded at -15 and +12 mV were not significantly different at $P < 0.2$, indicating a lack of discernable difference in the reversal voltages for the current under the three experimental conditions. *Inset (above)*: Steady-state current-voltage curves derived from the same measurements (cross-referenced by symbol).
(B) Current relaxation halftimes ($t_{1/2}$) as a function of voltage. Bars are means \pm SE from the same experiments (above) for 0 mM (solid), 1 mM (open) and 10 mM Mal (diagonal-hashed). *Inset*: Relaxation halftimes plotted relative to the control without Mal for 1 mM (●) and 10 mM (○) Mal.

Fig. 5. Internal OAA suppresses I_{Cl} in the presence of Mal in *Vicia* guard cells.

(A) Instantaneous anion current as a function of voltage as means \pm SE from 11 or more independent experiments for each combination of treatments. Measurements were carried out in 5 mM Ca^{2+} -MES buffer, pH 6.1, with 15 mM TEA-Cl and 15 mM CsCl. Guard cells were impaled with double-barrelled microelectrodes filled with 100 mM CsCl alone (●) and with additions 1 mM Mal without (○) and with 1 mM OAA (▼). Voltages clamped from a conditioning voltage of +40 mV to voltages between +40 and -220 mV in 10-s steps as in Fig. 1. *Inset (above)*: Steady-state current-voltage curves derived from the same measurements (cross-referenced by symbol).
(B) Current relaxation halftimes ($t_{1/2}$) as a function of voltage. Bars are means \pm SE from the same experiments (above) for 0 mM Mal and OAA (solid), 1 mM Mal without (open) and with 1 mM OAA (diagonal-hashed). *Inset*: Relaxation halftimes plotted relative to the control without additions for 1 mM Mal alone (●) and with 1 mM OAA (○).

Fig. 6. I_{Cl} in *Vicia* guard cells show a sensitivity to external Ac.

(A) Steady-state anion current as a function of voltage from 13 independent experiments as means \pm SE. Measurements were carried out in 5 mM Ca^{2+} -MES buffer, pH 6.1, with 15 mM TEA-Cl and 15 mM CsCl alone (●) and with additions of 1 mM (○) and 10 mM (▼) Ac. Voltages clamped from a conditioning voltage of +40 mV to voltages between +40 and -220 mV in 10-s steps as in Fig. 1. *Inset (above)*: Instantaneous current-voltage curves derived from the same measurements (cross-referenced by symbol).
(B) Current relaxation halftimes ($t_{1/2}$) as a function of voltage. Bars are means \pm SE from the same experiments (above) for 0 mM (solid), 1 mM (open) and 10 mM Ac (diagonal-hashed). *Inset*: Relaxation halftimes plotted relative to the control without Ac for 1 mM (●) and 10 mM (○) Ac.

Fig. 7. I_{Cl} in *Vicia* guard cells is suppressed by internal Ac.

(A) Steady-state anion current as a function of voltage from 15 or more independent experiments as means \pm SE. Measurements were carried out in 5 mM Ca^{2+} -MES buffer, pH 6.1, with 15 mM TEA-Cl and 15 mM CsCl alone (●) and with additions of 1 mM (○) and 10 mM (▼) Ac. Voltages clamped from a conditioning voltage of +40 mV to voltages between +40 and -220 mV in 10-s steps as in Fig. 1. *Inset (above)*: Instantaneous current-voltage curves derived from the same measurements (cross-referenced by symbol).
(B) Current relaxation halftimes ($t_{1/2}$) as a function of voltage. Bars are means \pm SE from the

same experiments (above) for 0 mM (solid), 1 mM (open) and 10 mM Ac (diagonal-hashed). *Inset*: Relaxation halftimes plotted relative to the control without Ac for 1 mM (●) and 10 mM (○) Ac.

Fig. 8. I_{Cl} in *Vicia* guard cells shows a high relative sensitivity to OAA (○) within the physiological concentration range compared with that for Mal (●). Mean \pm SE for I_{Cl} inactivation halftimes (A) and current amplitudes (B) determined as the complement values relative to the controls ($= 1 - X/X_0$) at -75 mV. Data were fitted independently by non-linear least-squares [22] to a hyperbolic function (solid curves) to derive apparent K_i values (see text).

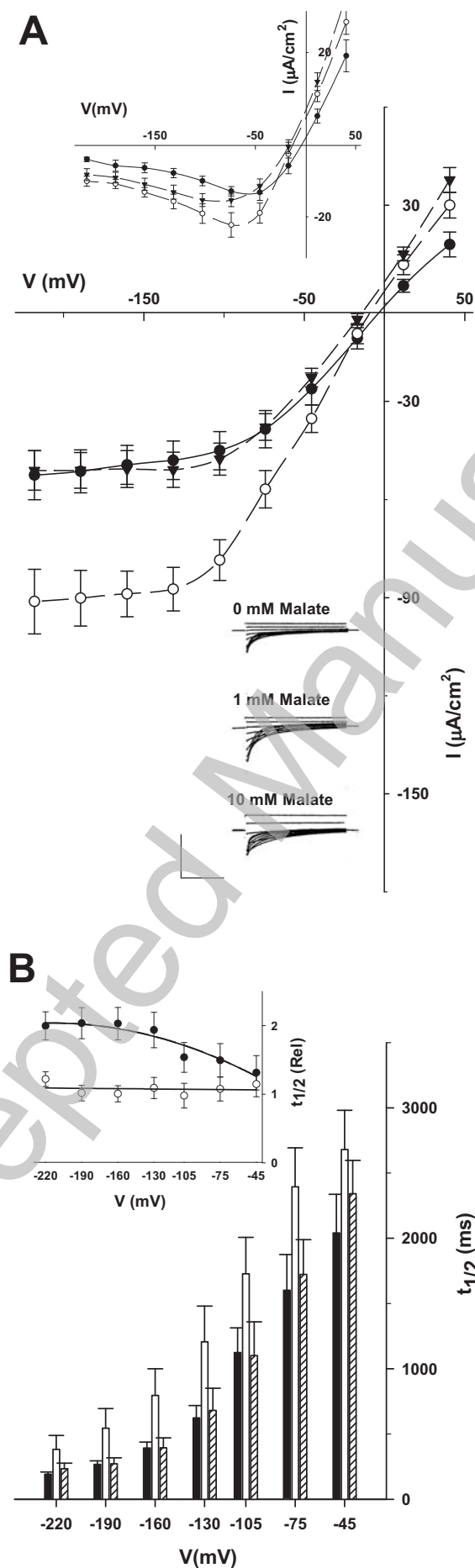


Fig1

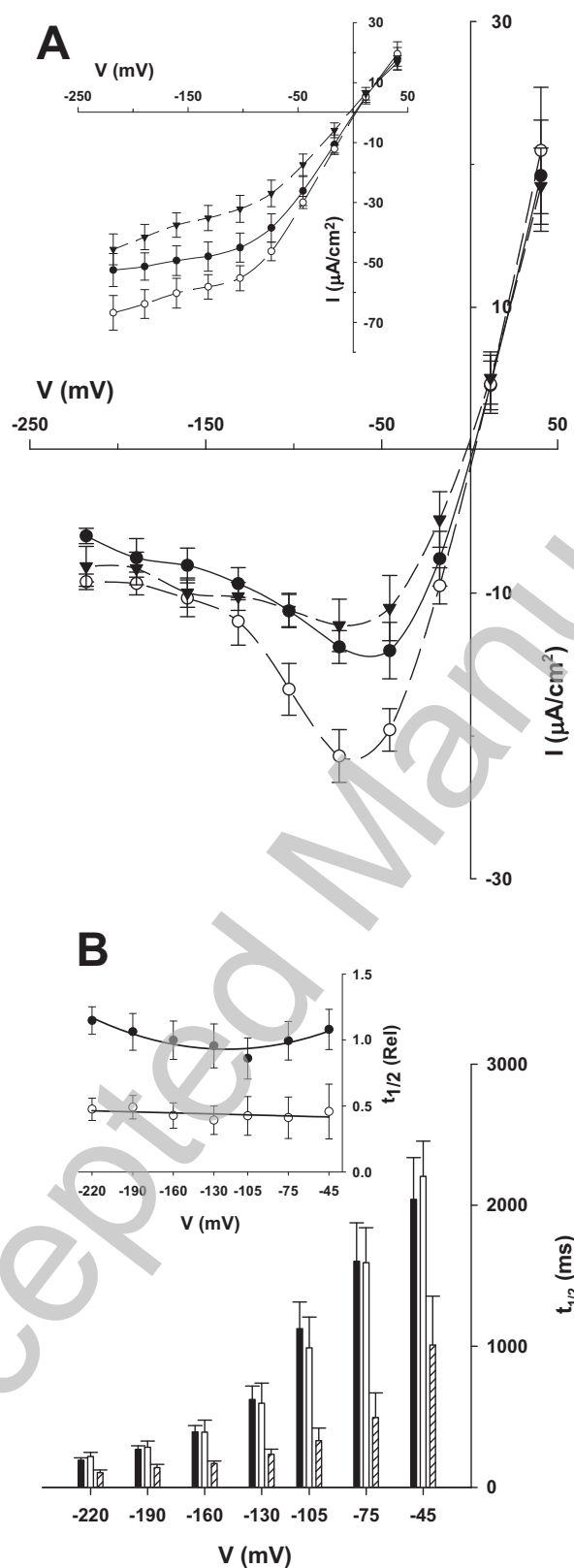


Fig 2

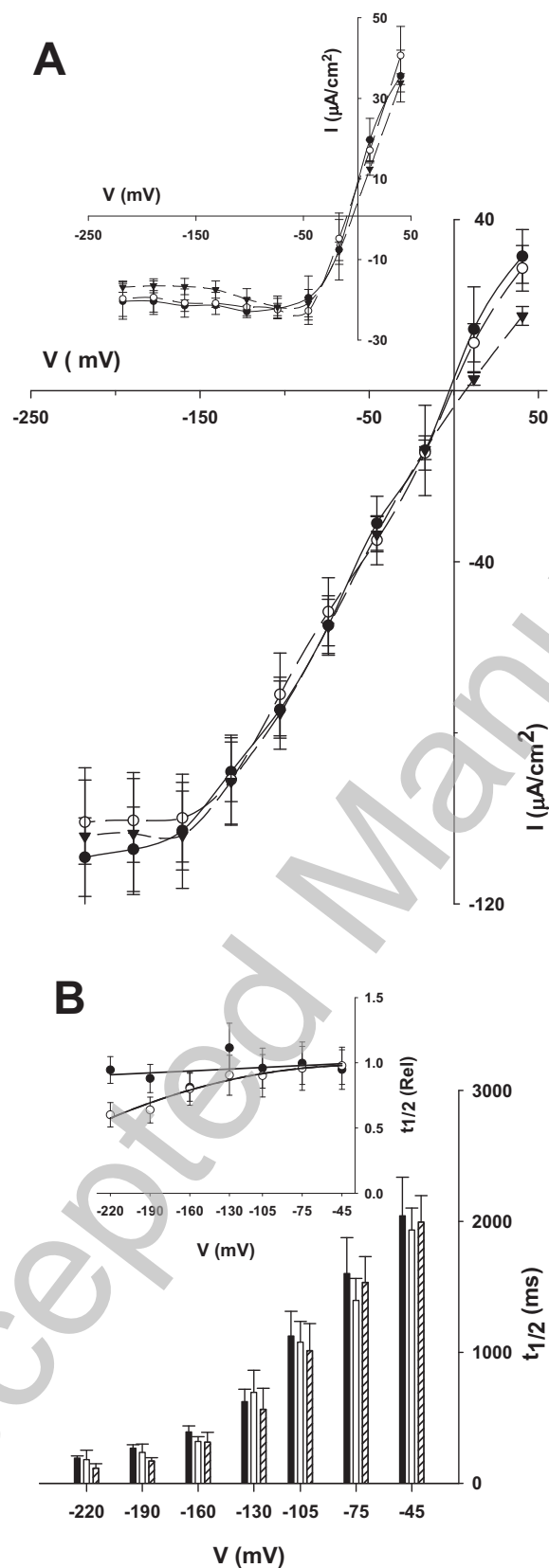


Fig 3

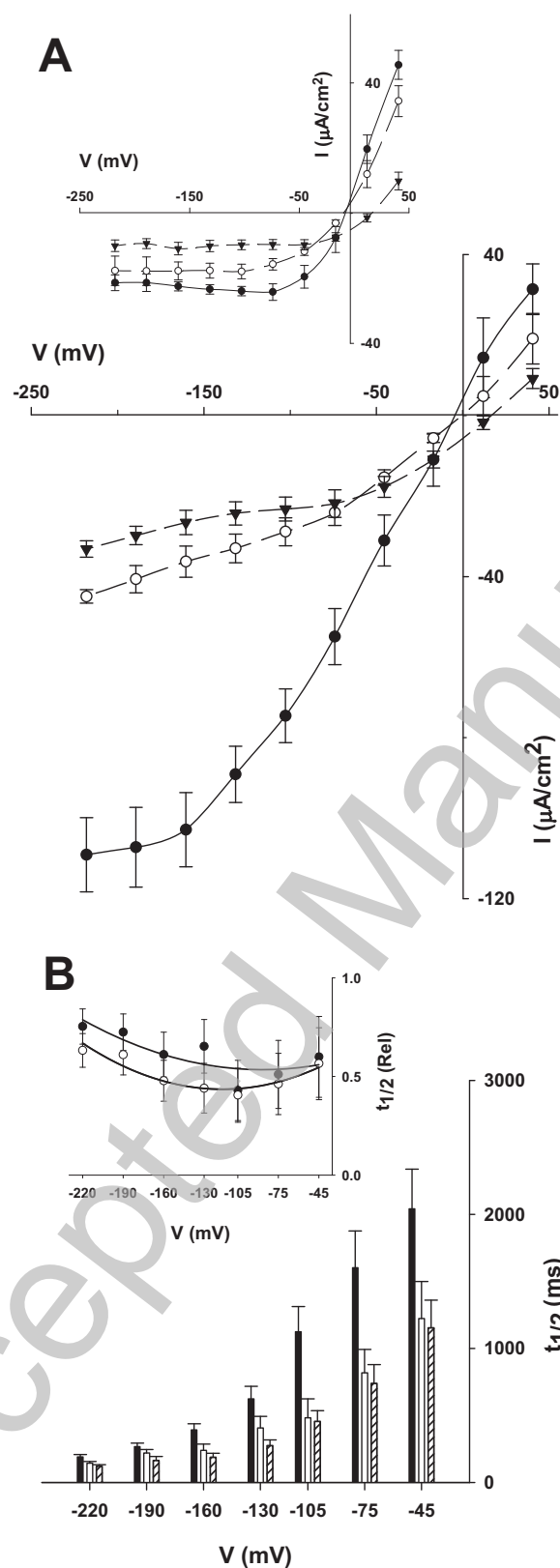


Fig 4

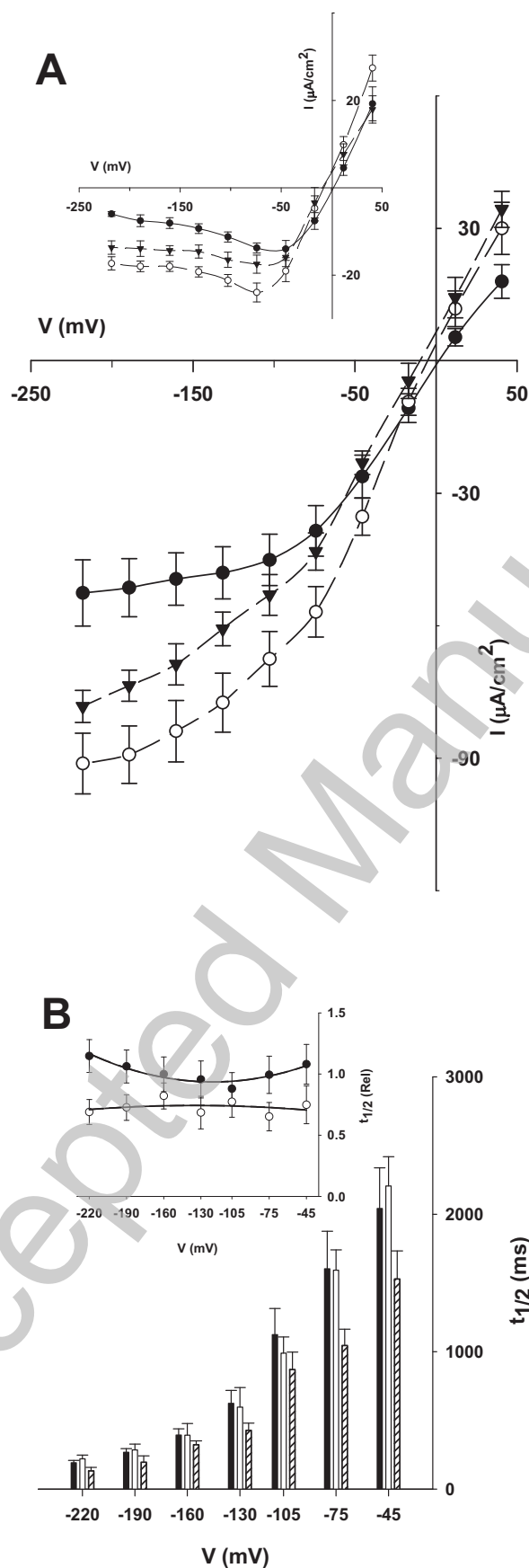


Fig 5

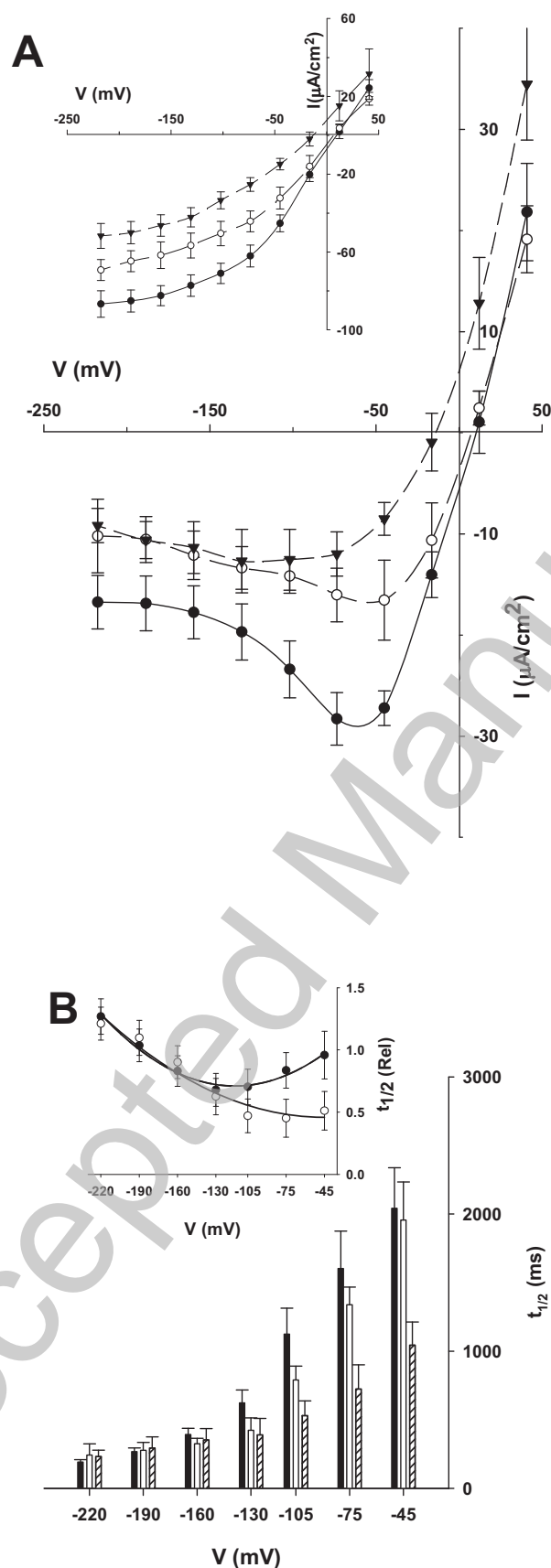


Fig 6

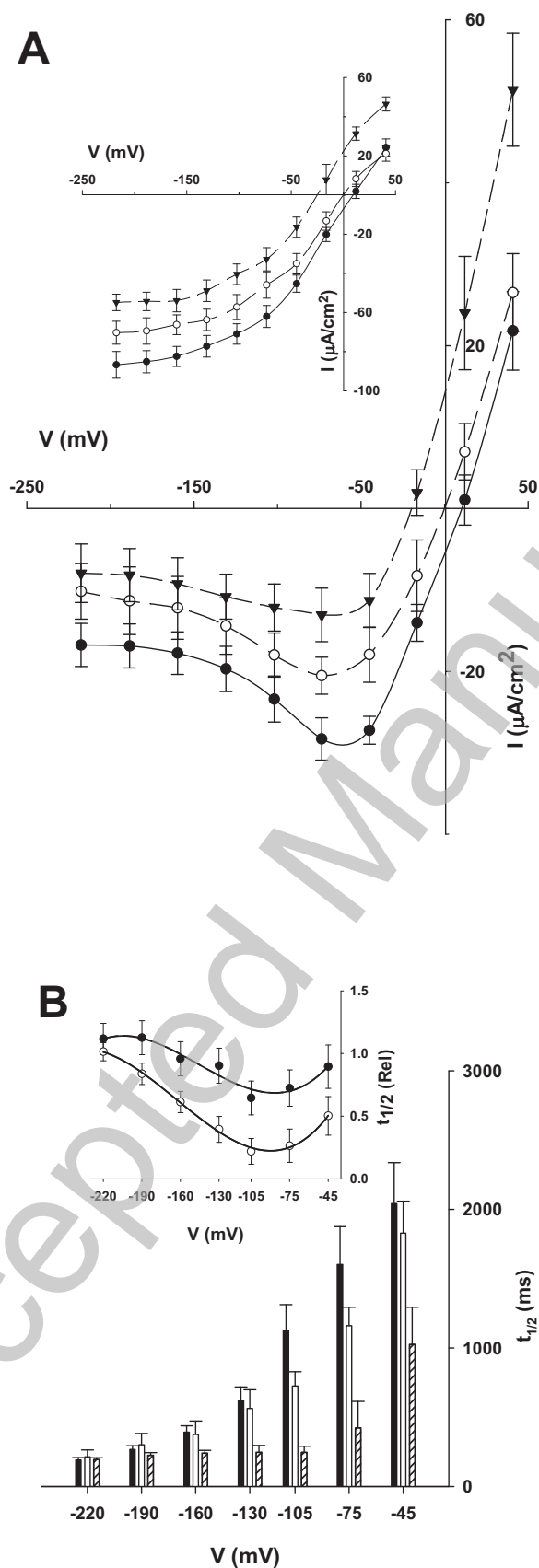


Fig 7

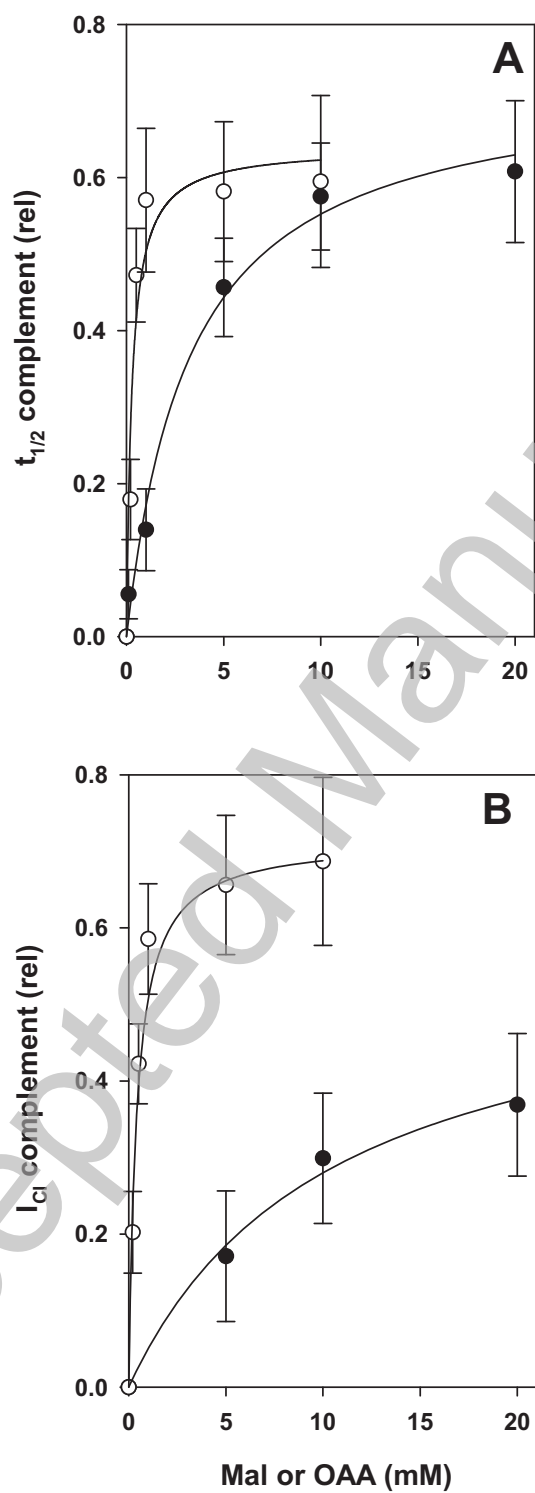


Fig 8